Optimization of the Angled Guide Plate for the Vossloh W14-PK Fastener

Wei Qi[1], Peyman Aela[2], Guoqing Jing[3], Yunyun Tong[4], Majid Movahedi Rad[5]

[1]School of Rail Transit, Chengdu Vocational & Technical College of Industry, No. 818, Zhengxing street, Tianfu New District, Chengdu Sichuan, P.R. China, 610218

[2] Department of Civil and Environmental Engineering, The Hong Kong Polytechnic University, 11 Yuk Choi Rd, Hung Hom, Kowloon, Hong Kong, China

[3] School of Civil Engineering, Beijing Jiaotong University, No. 3 Shangyuancun, Haidian District, Beijing, China, 100044

[4] School of Civil Engineering and Architecture, Zhejiang University of Science & Technology, 318 Liuhe Rd, Xihu Qu, Hangzhou, China, 310023

[5] Department of Structural and Geotechnical Engineering, Széchenyi István University, Egyetem tér 1, 9026 Győr, Hungary

e-mail: qw9199@my.swjtu.edu.cn, peyman.aela@polyu.edu.hk, gqjing@bjtu.edu.cn, 112013@zust.edu.cn, majidmr@sze.hu

Abstract: Angled guide plates are used to transmit the forces induced by trains, from the rail seat, to the concrete sleepers. Additionally, the design of the angled guide plates, with an appropriate width, supports tilting protection. Considering the updated requirements of the ML-1 railway line, in the Islamic Republic of Pakistan, an optimization design of the angled guide plate of the Vossloh W14-PK fasteners was carried out herein. The design requirements of the angled guide plate need to meet the requirements of structural stress and protect the plates from deterioration. Given the conducted refined model of the Vossloh W14 - PK fastener, it is shown that the force and deformation of the angled guide plate, in the bearing groove adjacent and the outside bolt hole area, are small. Therefore, it was preliminarily recommended that the optimization area of the angled guide plate be divided into the section I, close to the rail groove and section II, outside the bolt hole. The Finite Element Model (FEM) of angled guide plate was established, which is used to analyze the influences of length, width, depth and the number of holes, in section I and section II, on the force distribution, across the angled guide plate. The results show that the scheme of reducing the amount of material and minimizing the influence of force on the structure of the angled guide plate, is to punch three holes in section I and two holes in section II. The holes in section I/II are 20/30 mm in length, 8/8 in width, and 15/8 mm in depth,

respectively. The fatigue test showed that the optimized angled guide plate, had good application effects.

Keywords: Ballasted track; Fastening system; Angled guide plate; Structural design; Fatigue test

1 Introduction

The Islamic Republic of Pakistan will upgrade the railway line ML-1. This project mainly optimizes the ballasted trackbed, sleeper and fastener system. The research on ballast bed has a long history, including ballast crushing [1] [2], ballast bed settlement, ballast aggregate distribution, the force between the sleeper and track bed, ballast flight mechanism analysis, longitudinal and transverse resistance of trackbed, ballast screening, and reuse, etc [3-7]. The route selection scheme for different environments and grades is relatively mature, so the ballasted track of the ML-1 line can directly adopt existing standards.

Sleeper types of the ballasted track include wood sleeper, concrete sleeper, steel sleeper, composite sleeper, et al. The wooden sleeper has good elasticity and easy maintenance, but it has some problems, such as poor durability and unfavorable to environmental protection [8] [9]. Concrete sleepers have uniform quality, low cost, and an extensive application range [10]. Steel sleepers have corrosion, conductivity, and other problems, and are only used in special sections [11] [12]. Composite sleepers can use new materials and environmental protection materials to replace wooden sleepers, but now the cost is high [13] [14]. Therefore, concrete sleepers are suitable for ML1 line

The fastening system is a substantial track component to transfer train loads from the rail to the sleeper, minimize traffic-induced vibrations and impacts, maintain the rail inclination and track gauge, act as an electrical insulator between rails and sleepers, and provide adequate clamping force to rails to ensure lateral, longitudinal and torsional stability of rails [15]. As shown in Figure 1, the fastening system is a set of components, including screw spikes, pads, clips (clamps), insulators, and angled guide plates that connect the rails to sleepers in the track superstructure [16].

Due to the development of new types of railway sleepers and high-speed railways [17] [18], selecting the appropriate types of the fastening system is one of the important issues that should be taken into account. Given that the two terms of structural design and flexibility, railway fastenings are divided into direct/indirect and rigid/elastic types, respectively [19].

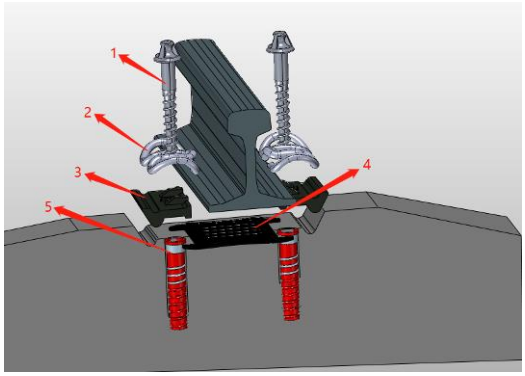

Figure 1
Composition of Vossloh W14-PK fasteners1-Bolt studs, 2-Fastening clip, 3- Angled guide plate, 4-Rail pad, 5-Preburied casing

As shown in Figure 2, the direct fastenings connect the rail directly to the sleeper through rail pads without using baseplates, while indirect fastenings connect the rail to the sleeper through the rail pad and baseplate pad [20]. The application of direct fastenings causes rail seat deterioration as the consequence of shock loads on loosened fastening clips (Figure 3), while the application of indirect fastenings led to a pulsating force distribution and fluctuating around the initial tension value that prolongs the railway superstructure service life [21]. On the other hand, fastenings could be classified into rigid or elastic types. The rigid fastenings were a common system used in the early 1900s for bolting the rail to the timber sleeper rigidly, whereas the screws are tightened in an elastic rail fastening such that an initial tension is formed through the elastic clip or the spring washers, which allows a slight rail movement within the rail seat. Loosening of rigid fastenings after a relatively short period of operation is the principal disadvantage of this type, which led to over-stressing the clips under high lateral forces and consequential damages of the fastening clips.

The anchorage of the fastening system in the sleeper has an important role in joining the elastic clip or spring part of the assembly to the less resilient sleeper. It should be able to tolerate impact loads and vibration transmitted to the sleeper without cracking or loosening it. While polypropylene and HDPE have been used in the past for light-duty applications, anchorages for threaded fastenings are typically made of nylon or composite materials. To avoid damage in freezing weather, care must be taken to expel any water during the assembly of the fastening. Shoulders for non-threaded fastenings are usually made of ductile cast iron, such as, S.G. Iron (Spheroidal Graphite Iron).

Figure 2
(a) Direct rigid fastening, (b) indirect rigid fastening, (c) direct elastic fastening,
(d) indirect elastic fastening [19] [20]

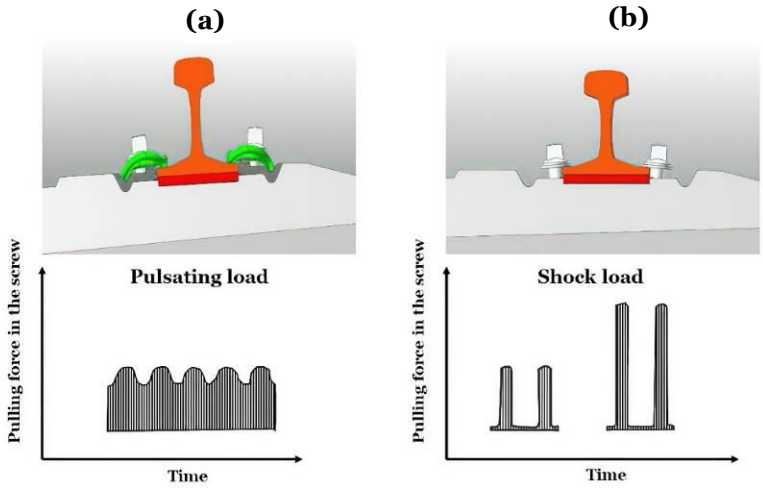

Figure 3
Pulling load distribution for (a) elastic and (b) rigid fastening

The shape of the concrete-encased portion of the shoulder has been refined over time to ensure that it extends down into the prestressed region of the sleeper and securely transmits lateral and torsional forces. Each part of the fastening cast into the sleeper must be able to withstand a 60 kN pullout force without causing damage to the sleeper.

A repeated loading test is a suitable method to evaluate the long-term performance of fasteners subjected to traffic loading caused by passing trains. In this regard,

cyclic loading is applied to the railhead so that the position of applying load is depending on fastening vertical stiffness, track axle load, and curvature. The cyclic load could be applied to an individual rail or both rails on a concrete sleeper, as shown in Figure 4a-b. For non-symmetrical fastening systems, the rail should be fixed between two sleepers or half sleepers. The repeated load could be applied vertically or obliquely depending on the support position (Figure 4c-d). The requirements of British and AREMA standards for conducting repeated load tests are compared in Table 1.

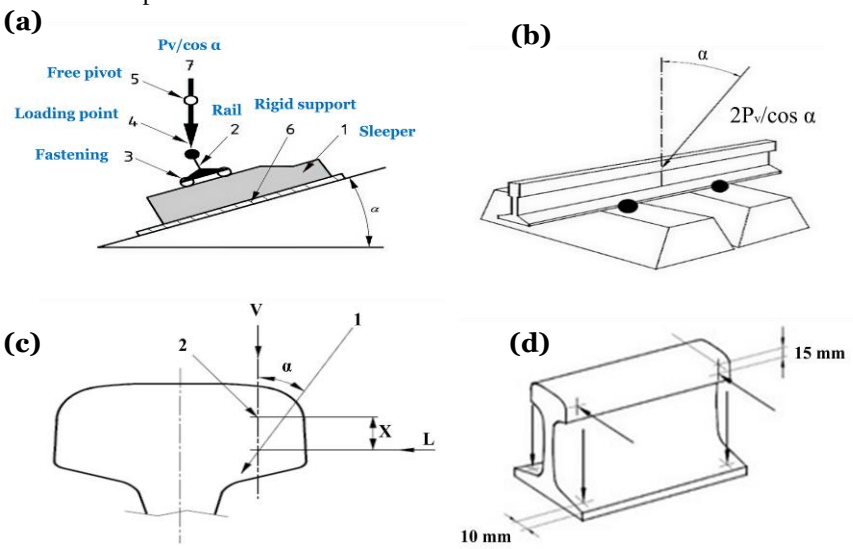

Figure 4

Laboratory tests conditions: (a-b) Repeated load test arrangements, (c) Loading point on the railhead, (d) Displacement measurement positions [22]

Table 1

Repeated loading test requirements according to different standards

BS EN 13481-2	AREMA 1-30
The minimum rail length is 500 mm.	The rail length should be 457 mm – 508 mm.
The clamping force is determined after the test according to BS EN 13146-7.	The uplift force is determined according to Article 2.6.1.
The magnitude and position of load are associated with the track axle load and curve radius presented in Table 4 and Figure 4a-b. Cyclic loading should be continued up to 3×10^6 cycles at a frequency of (4 ± 1) Hz.	The cyclic loading is applied at the angle of 20˚ relative to the vertical axis of the rail for 3×10^6 cycles at a frequency of 2.5 Hz. The magnitude of upward loading should be 0.6P, and downward load should be 0.6P + 133.5 kN or 133.5 kN if a single spring/hydraulic ram or double-acting hydraulic ram is used, respectively.

The maximum temperature of fastening components should be lower than 50˚C.	The maximum temperature of the rail pad should be lower than 71˚C.
The maximum loading rate should be 200 kN/min for a single sleeper.	The maximum loading rate should be 22.24 kN/min for a single sleeper.

In this paper, the long-term performance of W14-PK fasteners was the main concern since the Islamic Republic of Pakistan will upgrade the railway line ML-1. with Vossloh W14-PK fasteners, which is a suitable alternative for ballasted tracks. The fastening system modification requirements for the angled guide plate, are as follows:

(1) It must fulfill requirements for ballasted track lines with gauge 1676 mm

(2) It should be capable of connecting 60E1 to 54E1 rails

(3) It should be able to be supported by China IIIa prestressed concrete sleeper with shoulder retaining

(4) It can save material while satisfying the force of the angled guide plate

2 Materials and Methods

2.1 Materials

Pakistan ML-1 railway line adopts 54E1 rail and 60E1 rail. The rail material is 350HT. It is a non-porous rail with a length of 25 m. The weight of a rail per meter is 60.21 kg. Its elastic modulus is 210 GPa, the Poisson's ratio is 0.3 and the density is 7830 kg/m^3.

The fastener clip is type ω. Its buckle pressure is 10 KN. Its material is 38Si7. Its elastic modulus is 200 GPa, the Poisson's ratio is 0.3, and the density is 7830 kg/m^3. Figure 5 is the dimension of the angled guide plate. Angled guide plate material is glass fiber reinforced PA66/PA6. Its elastic modulus is 9.6 Gpa, the Poisson's ratio is 0.35 and the density is 1150 kg/m^3. Table 2 is its physical parameters.

Table 2

Physical parameters of the angled guide plate

No.	Item	Unit	Index
1	Tensile strength (23℃)	MPa	≥170
2	Tensile strength (70℃)	MPa	≥110
3	Elongation at break (23℃)	%	≤4
4	Elongation at break (70℃)	%	≤7

5	Bend strength (23℃)	MPa	≥250
6	Bend strength (70℃)	MPa	≥140
7	Volume resistivity (wet state)	Ω·cm^3	≥10^{10}
	Volume resistivity (dry state)	Ω·cm^3	≥10^{14}
8	Non-notched impact strength（23°C）	KJ/m²	≥80

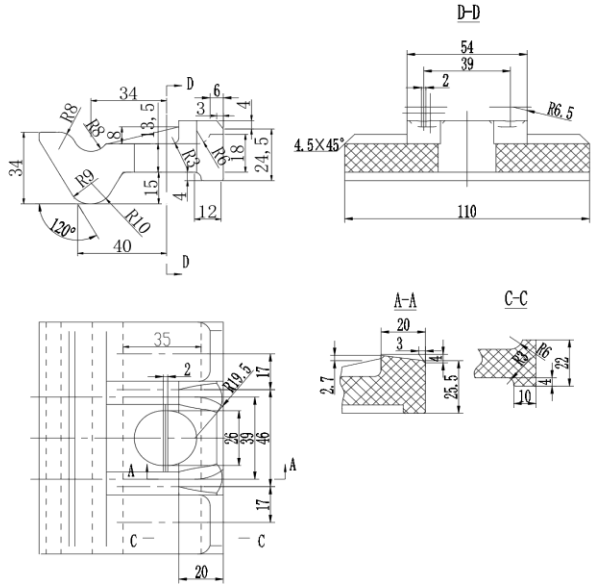

Figure 5
Structural details of the angled guide plate

The material of the rail pad is the CPU. Its strength is 80 kN/mm (23 °C) and its stiffness variation is less than 30% at 70°C. Its elastic modulus is 5 GPa, the Poisson's ratio is 0.4 and the density is 1200 kg/m^3.The bolt studs material is high-quality carbon steel or alloy structural steel. Its strength grade is 5.6. The elastic modulus of the bolt studs is 220 GPa, the Poisson's ratio is 0.3, the density is 7830 kg/m^3 force is 75 kN. The sleepers' strength grade of concrete should not be less than C60. The elastic modulus is 36 GPa, the Poisson's ratio is 0.2, and the density is 2400 kg/m^3.

2.2 Model

2.2.1 Load

Load value is determined according to the Chinese railway track design code (TB 10098-2017). The dynamic load of the wheel is expressed by the maximum

possible value of the equivalent static load. The vertical equivalent static load on a straight track is shown in Eq. (1).

$$\begin{cases} v \le 120km/h & P_d = P_0(1+\alpha) \\ 120km/h < v \le 160km/h & P_d = P_0(1+\alpha+\beta)(1+\alpha_1) \end{cases} \quad (1)$$

P_d: the vertical equivalent static load of wheel acting on the rail (kN)

P_0: static wheel weight (kN)

N: Driving speed (km / h)

α,α_1: speed coefficient, α=0.6v/ 100, α_1=0.3 Δv 1/100

β: Partial load coefficient

$$\beta = \frac{2 \cdot \Delta h \cdot H}{S^2} \quad (2)$$

Δh: unbalanced superelevation (mm)

H: height of the center of gravity of locomotive or vehicle (mm)

S: center distance between inner and outer rails (mm)

According to the design parameters, the Pakistan railway has the highest running speed of 160 km/h, axle load of 25 t, and a track gauge of 1676 mm. It can be seen from this that the velocity coefficient α = 0.72， α_1 = 0.12, partial load coefficient β = 0.12. The static load on the sleeper is about 40% of the axle load. Therefore, the vertical load P_d of dynamic wheel load is 103.04 kN. The lateral force is 0.8 P_d according to the Chinese Railway Track Design Code, so, P_l = 82 kN

$$P_d = P_0(1+\alpha+\beta)(1+\alpha_1) = 125000 \times 0.4 \times 1.84 \times 1.12 = 103040N \quad (3)$$

2.2.2 Analytical Model

The angled guide plate is one of the fastening system components, and its stress is mainly affected by the one-sided rail row. In order to optimize the angled guide plate, a finite model of the fastener system under a single rail is established, as shown in Figure 6. The finite element model is used to analyze the influence of the length, width, depth, and the number of holes in section I and section II on the force distribution across the angled guide plate, as shown in Figure 7. The dimensions of length, width, depth, and the number of holes were set according to the specific conditions of the optimization area. The optimum design scheme is shown in Table 3.

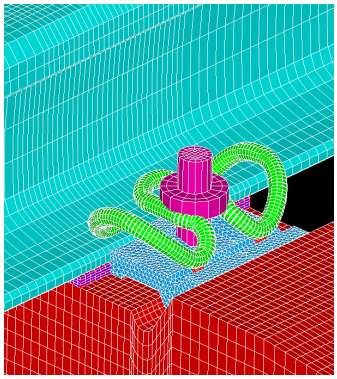

Figure 6
Fine finite element model of fastener system

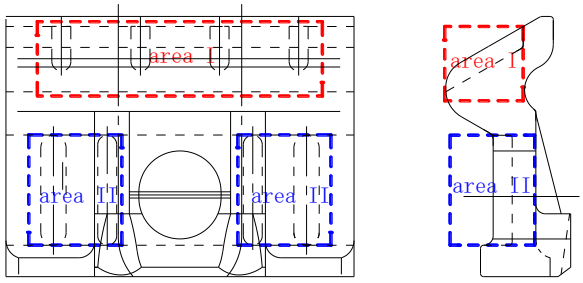

Figure 7
Hole area division of the angled guide plate

Table 3
The optimum design scheme of the angled guide plate

	No.	Number of holes	Variable	Dimension （Unit: mm）	Abbreviation
Section I	1	3	length	5,10,15,20	I-3-l
	2	3	width	4,8,12	I-3-w
	3	3	depth	5,10,15,20,25	I-3-d
	4	1	length	5,10,15	I-1-l
	5	1	width	20,30,40	I-1-w
	6	1	depth	10,15,20	I-1-d
Section II	7	2	length	20,25,30,35	II-2-l
	8	2	width	4,8,12,16	II-2-w
	9	2	depth	4,8,12	II-2-d

2.3 Test Method

2.3.1 Static Test

Static test including hardness, drainage rate, internal porosity, insulation resistance, compression resistance. Hardness is measured by the Brinell hardness tester [23].

The drainage rate test was to allow the gauge baffle to absorb water for 12 hours. Record the weight as the initial weight W_1. Place the angled guide plate in the heating furnace at 120 ± 3 ℃ for 2 hours and then weigh it within three minutes, after taking it out, then record the weight as W_2. See Eq. (4) for drainage rate P.

$$P = \frac{W_1 - W_2}{W_1} \times 100\% \tag{4}$$

The internal porosity was to cut the gauge stop into four pieces along the longitudinal direction, and then detect whether there had porosity inside [24]. The insulation resistance test was completed by a high resistance tester. The angled guide plate was boiled for 2 h, then, wiped the surface moisture with filter paper quickly after taking it out. Aluminum foil was padded on the upper and lower planes of the gauge baffle, and electrodes were placed respectively. After the gauge baffle was placed stably, measured its resistance under 500 V DC voltage [24]. The compressive performance test was to place the mounting frame together with the gauge baffle on the testing machine (Figure 8). Add to 60 kN at the loading speed of 0.5 kN/s, and unload after stabilizing for 10 s. After repeating this three times, remove the mounting frame together with the angled guide plate from the testing machine. The gauge baffle was taken out and placed on the measuring platform to measure its depth of camber.

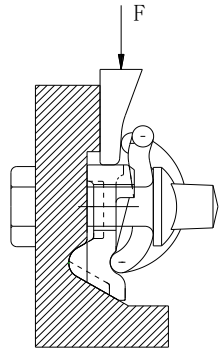

Figure 8
Compressive performance test

2.3.2 Fatigue Test

The fatigue test device is shown in Figure 9. Before the fatigue test, slowly load the test assembly system to the maximum load. The loading rate was 200 kN/min. Repeat the loading 10 times. During the last 3 times of loading, the error of the included angle between the maximum load action line and the vertical line of the rail bottom was within ± 0.5°. Apply fatigue load to the test fastener assembly. The minimum load was 9 kN and the maximum load was 500 kN. Unload after 3×106 load cycles, and let the fastener parts for the test stand for 24 h. Then, test rail longitudinal resistance, insulation performance, and uplift resistance of embedded parts.

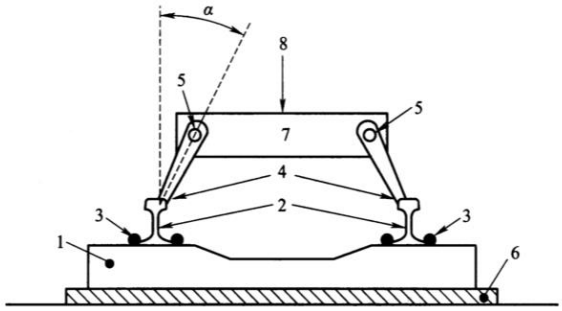

Figure 9

The fatigue test device: 1-sleeper; 2-steel rail; 3-fastener system; 4-loading device; 5-pivot; 6-cushion on rigid foundation; 7-booster frame; 8-Maximum acting load, 500 kN

3 Results and Discussion

3.1 Analysis of Angled Guide Plate

In the three-dimensional direction, the original angled guide plate has small displacement under train load, see Table 3. The displacement of the angled guide plate in the X direction is larger than that in other directions under train load. Three-dimensional stresses under train loads satisfy the requirements, see Table 4. The tensile and compressive stress in the X direction is greater than that in other directions. The principal stress of the angled guide plate is shown in Table 5. The maximum tensile stress of the angled guide plate is 39.4 MPa, which is 35.82% of the allowable stress of the material. The angled guide plate has more material safety margins, and its structure has a larger optimization space.

Table 4

Three-dimensional displacement of angled guide plate under load (Unit: mm)

displacement of X		displacement of Y		displacement of Z	
Max	Min	Max	Min	Max	Min
1.58E-3	-1.10E-1	2.06E-2	-1.13E-2	7.68E-3	-4.36E-2

Table 5

Three dimensional stress of angled guide plate under load (Unit:MPa)

Stress of X		Stress of Y		Stress of Z	
Max	Min	Max	Min	Max	Min
37	-36.4	13.2	-24.8	21.2	-15.5

Table 6

Principal stress of angled guide plate under load (Unit: MPa)

1st principal stress		2nd principal stress		3rd principal stress	
Max	Min	Max	Min	Max	Min
39.4	-14.5	13.2	-24.9	8.84	-36.5

3.2 Analysis Scheme

- Comparison of results under condition I-3-l

Under conditions I-3-l，with the increase of the hole length, most of the stress and displacement of the angled guide plate increase. Except that the displacement in direction Y is greatly affected by the opening length, the variation of most indexes by the increase of opening length is not greater than 50% (Figure 10).

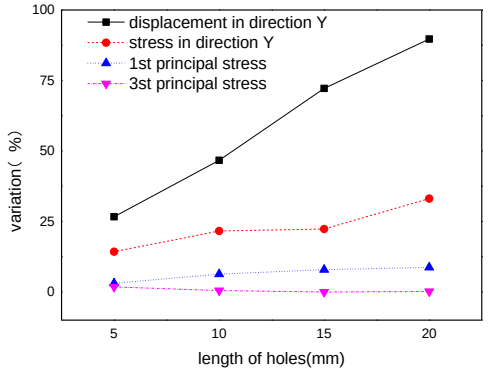

Figure 10

Variation of deformation and stress under condition I-3-l

- Comparison of results under condition I-3-w

Under condition I-3-w，with the increase of the hole width, most of the stress and displacement of the angled guide plate increase. When the hole width exceeds 8mm, the parameters of the angled guide plate increase rapidly (Figure 11).

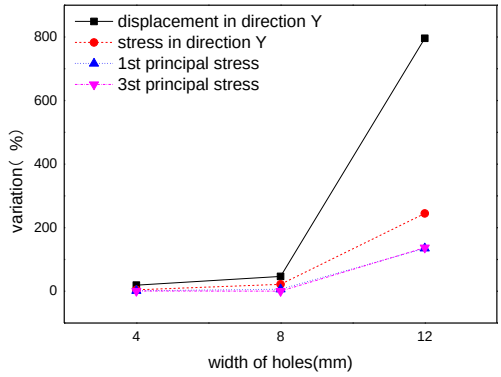

Figure 11
Variation of deformation and stress under condition I-3-w

- Comparison of results under condition I-3-d

Under condition I-3-d, with the increase of the hole depth, most of the stress and displacement of the angled guide plate increase. When the hole depth exceeds 15mm, the parameters of the angled guide plate increase rapidly (Figure 12).

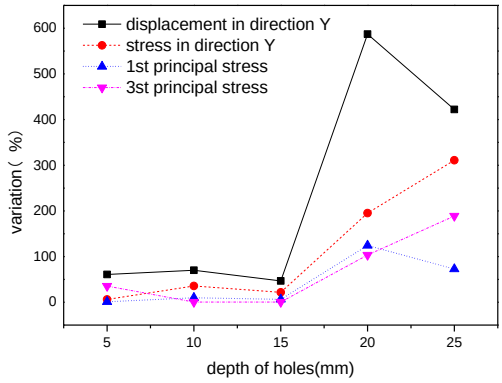

Figure 12
Variation of deformation and stress under condition I-3-d

- Comparison of results under condition I-1-l

Under the condition of a single hole in area I, the stress and displacement parameters of the angled guide plate increase significantly (Figure 13). With the

increase of hole length, the stress on the angled guide plate decreases. However, the variation of each parameter of the angled guide plate exceeds more than 80%.

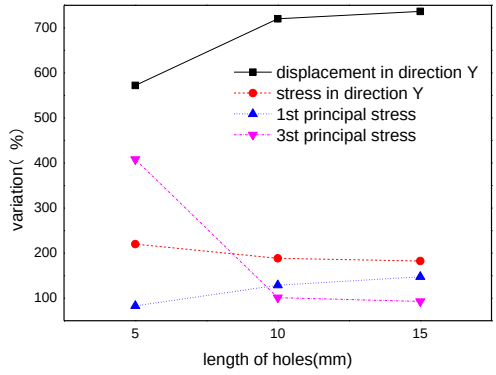

Figure 13
Variation of deformation and stress under condition I-1-l

- Comparison of results under condition I-1-w

Under the condition of a single hole in area I, the stress and displacement parameters of the angled guide plate increase significantly with the width of the hole increase (Figure 14). The displacement in direction Y increases most significantly.

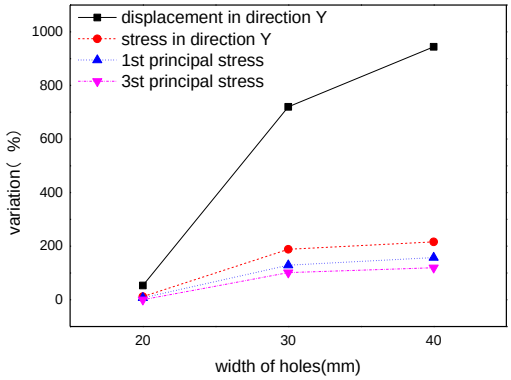

Figure 14
Variation of deformation and stress under condition I-1-w

- Comparison of results under condition I-1-d

Under the condition of a single hole in area I, the stress and displacement parameters of the angled guide plate increase significantly with the depth of the hole increase (Table 15). The displacement in direction Y increases most significantly.

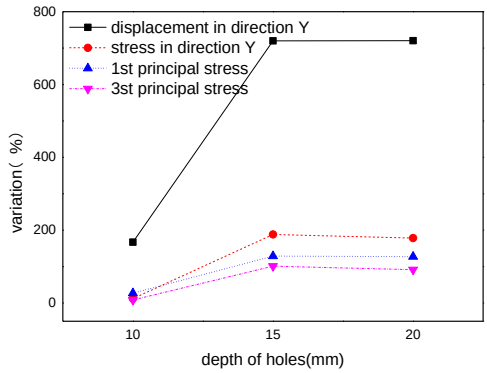

Figure 15
Variation of deformation and stress under condition I-1-d

- Comparison of results under condition II-2-l

Under the condition of two holes in area II, the increase of hole length has little effect on the stress and displacement of the angled guide plate (Figure 16). It was found that only when the length of the hole reaches 35 mm, the displacement in the Y direction exceeds 36%.

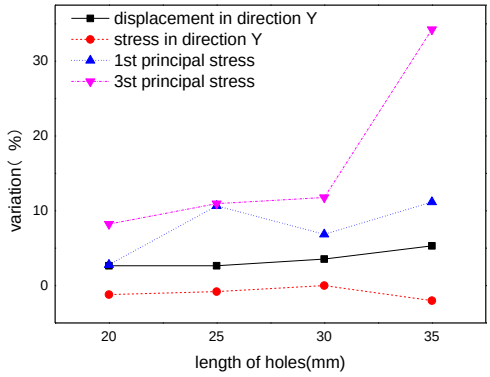

Figure 16
Variation of deformation and stress under condition II-2-l

- Comparison of results under condition II-2-w

Under the condition of two holes in area II, the stress and displacement of the angled guide plate increase with the hole width increase. When the hole width exceeds 12 mm, the parameters of the angled guide plate increase significantly (Figure 17).

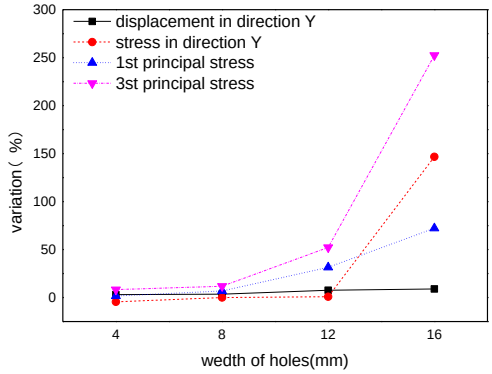

Figure 17
Variation of deformation and stress under condition II-2-w

- Comparison of results under condition II-2-d

Under the condition of two holes in area II, the increase of hole depth has little effect on the stress and displacement of the angled guide plate (Figure 18). Only when the hole depth reaches 12 mm, the 3rd principal stress exceeds 37%.

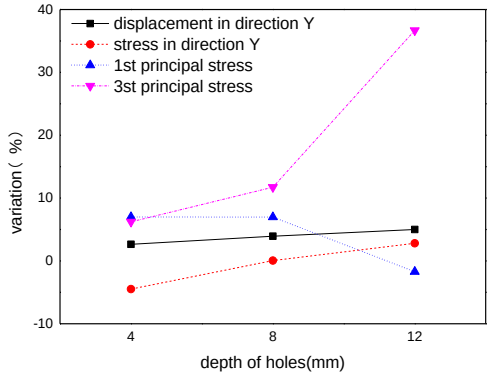

Figure 18
Variation of deformation and stress under condition II-2-d

3.3 Optimization Scheme

By comparing the displacement and stress variation of angled guide plates under different schemes, it can be seen that the effect of the single-hole scheme is poor. According to the spatial distribution, deformation, and stress variation of the angled guide plate's two areas, the optimal design scheme of the angled guide plate is: Area I uses three holes with 20 mm long, 8 mm wide, 15 mm deep.

Area II uses two holes 30 mm long, 8 mm wide, 8 mm deep. The deformation and stress variation of the angled guide plate in this scheme is shown in Table 7~ Table 9. The displacement and stress of the angled guide plate had little variation. This realizes the purpose of ensuring the safety of angled guide plate structure and saving materials.

Table 7

Three-dimensional displacement variation of angled guide plate under load (Unit: mm)

displacement of X		displacement of Y		displacement of Z	
Max	Min	Max	Min	Max	Min
22.60%	13.53%	37.99%	93.89%	63.29%	-1.97%

Table 8

Three-dimensional stress variation of angled guide plate under load (Unit: MPa)

Stress of X		Stress of Y		Stress of Z	
Max	Min	Max	Min	Max	Min
18.47%	8.34%	7.86%	32.75%	9.26%	15.54%

Table 9

Principal stress variation of angled guide plate under load (Unit: MPa)

1st principal stress		2nd principal stress		3rd principal stress	
Max	Min	Max	Min	Max	Min
19.04%	6.35%	7.77%	-0.13%	-7.64%	15.64%

3.4 Test Results

Through static load test and fatigue load test, it is proved that all indexes of the optimized gauge baffle meet the applicable requirements. The results are shown in Table 10 and Table 11.

Table 10

The test results of the angled guide plate

No.	item	unit	standard	test result
1	hardness	HRR	≥105	112
2	Drainage rate	%	Drainage rate of angled guide plate after water absorption modulation shall be ≥ 0.4%	0.85
3	internal porosity	/	There should be no bubbles or voids inside	no bubbles or voids inside

4	Insulation resistance	kΩ	$\geq 5\times10^6$	1.91×10^9
5	compression resistance	/	Angled guide plate shall not be damaged after the compression test, and its uplift value shall not exceed 0.5 mm	no damage and uplift value is 0.3 mm

Table 11

Fatigue test results of the fastener assembly

No.	item		unit	standard	test result
1	Rail longitudinal resistance		kN	≥9	12.1
2	Insulation performance		kΩ	≥5	7.6
3	Uplift resistance of embedded parts		kN	≥100	After the 100kN pullout test, the embedded parts were not damaged, concrete around embedded parts without visible cracks and mortar peeling
4	Assembly fatigue performance	Component state after fatigue	/	Components should not be damaged	No damage to components
5		Variation of track gauge expansion	%	≤6	3.9
6		Variation of rail longitudinal resistance	%	≤20	9.1
7		Variation of assembly buckle pressure	%	≤20	9.4
8		Static stiffness variation of assembly	%	≤25	13.2

Conclusions

The angled guide plate of the Vossloh w14-pk fastener has a large safety margin, under the actions of train loads and exhibits optimization space.

We divided the angled guide plate into Area I, close to the rail groove and Area II, outside the bolt hole. The angled guide plate was then optimized by the placement of holes. The optimization scheme, after the theoretical analysis, is to provide holes in Area I, 20 mm long, 8 mm wide and 15 mm deep, and holes in Area II

that are 30 mm long, 8 mm wide and 8 mm deep. This achieved the goal of ensuring the safety of angled guide plate structure and te economy of material use.

The fatigue test of the optimized angled guide plate showed that the optimized scheme met or or in most cases, exceeded the applications, standard minimal requirements.

Acknowledgement

This work was supported by the Natural Science Foundation of Zhejiang Province (Grant No. LY19E080002).

References

[1] Y. Guo, V. Markine, X. Zhang, W. Qiang, and G. Jing, "Image analysis for morphology, rheology and degradation study of railway ballast: A review," *Transp. Geotech.*, 2019

[2] E. Juhász and S. Fischer, "Investigation of railroad ballast particle breakage," *Pollack Period.*, Vol. 14, No. 2, pp. 3-14, 2019

[3] Y. Guo, V. Markine, J. Song, and G. Jing, "Ballast degradation: Effect of particle size and shape using Los Angeles Abrasion test and image analysis," *Constr. Build. Mater.*, Vol. 169, pp. 414-424, 2018

[4] Y. Guo, H. Fu, Y. Qian, V. Markine, and G. Jing, "Effect of sleeper bottom texture on lateral resistance with discrete element modelling," *Constr. Build. Mater.*, Vol. 250, p. 118770, 2020, doi: https://doi.org/10.1016/j.conbuildmat.2020.118770

[5] G. Jing, D. Ding, and X. Liu, "High-speed railway ballast flight mechanism analysis and risk management–A literature review," *Constr. Build. Mater.*, Vol. 223, pp. 629-642, 2019

[6] G. Jing, P. Aela, H. Fu, and M. Esmaeili, "Numerical and Experimental Analysis of Lateral Resistance of Bi-Block Sleeper on Ballasted Tracks," *Int. J. Geomech.*, 2020

[7] W. Jia, V. Markine, Y. Guo, and G. Jing, "Experimental and numerical investigations on the shear behaviour of recycled railway ballast," *Constr. Build. Mater.*, Vol. 217, pp. 310-320, 2019, doi: https://doi.org/10.1016/j.conbuildmat.2019.05.020

[8] A. M. Zarembski, "Concrete vs. wood ties: Making the economic choice," 1993

[9] P. Qiao, J. F. Davalos, and M. G. Zipfel, "Modeling and optimal design of composite-reinforced wood railroad crosstie," *Compos. Struct.*, Vol. 41, No. 1, pp. 87-96, 1998

[10] W. Ferdous, A. Manalo, G. Van Erp, T. Aravinthan, S. Kaewunruen, and A. Remennikov, "Composite railway sleepers–Recent developments, challenges and future prospects," *Compos. Struct.*, Vol. 134, pp. 158-168,

2015

[11] P. A. Guoqing Jing Hao Fu, "The Contribution of Ballast Layer Components to the Lateral Resistance of Ladder Sleeper Track," *Constr. Build. Mater.*, Vol. (under rev, 2018

[12] W. Ferdous and A. Manalo, "Failures of mainline railway sleepers and suggested remedies–review of current practice," *Eng. Fail. Anal.*, Vol. 44, pp. 17-35, 2014

[13] A. Manalo, T. Aravinthan, W. Karunasena, and A. Ticoalu, "A review of alternative materials for replacing existing timber sleepers," *Compos. Struct.*, Vol. 92, No. 3, pp. 603-611, 2010, doi: https://doi.org/10.1016/j.compstruct.2009.08.046

[14] E. R. Anne, "Rubber/plastic composite rail sleepers," *UK waste Resour. action Program.*, 2006

[15] S. Fischer, B. Eller, Z. Kada, A. Németh, "Railway Construction," Univ. Nonprofit Kft, Győr, 2015, 334 p.

[16] Vossloh, "Sleeper anchor SN," 2015 [Online] Available: http://www.vossloh.com

[17] G. Jing, M. Siahkouhi, J. Riley Edwards, M. S. Dersch, and N. A. Hoult, "Smart railway sleepers - a review of recent developments, challenges, and future prospects," *Constr. Build. Mater.*, Vol. 271, p. 121533, 2021, doi: https://doi.org/10.1016/j.conbuildmat.2020.121533

[18] M. J. G. Romero, J. R. Edwards, C. P. L. Barkan, B. Wilson, and J. Mediavilla, "Advancements in fastening system design for North American concrete crossties in heavy-haul service," 2010

[19] A. Sładkowski and K. Bizoń, "Aspects of Rail Infrastructure Design," in *Sustainable Rail Transport*, Springer, 2018, pp. 113-145

[20] I. Grossoni, Y. Bezin, and S. Neves, "Optimisation of support stiffness at railway crossings," *Veh. Syst. Dyn.*, Vol. 56, No. 7, pp. 1072-1096, 2018

[21] J. Liu, "Influence of the rail fastening components on the lateral deformation and load distribution behavior of the rail." Technische Universität München, 2013

[22] E. 13146-4:2020 Standardization, E. C. f., "Railway applications - Track - Test methods for fastening systems - Part 4: Effect of repeated loading.," *CEN*, 2020

[23] inspection and quarantine of the people's republic of china General administration of quality supervision, "plastics-determination of hardness-part 2. Rockwell hardness," *GB T 3398.2*, 2008

[24] C. N. R. Administration, "Fastening systems for high-speed railway-Part 3 : Type V fastening system," *TB/T 3395.3*, 2015